Strong strain-dependent elastic stiffness in ultrathin Pt films on MgO

N. Nakamura,[a] Y. Kake, H. Ogi, and M. Hirao
Graduate School of Engineering Science, Osaka University, 1-3 Machikaneyama, Toyonaka, Osaka 560-8531, Japan

(Received 14 January 2010; accepted 8 June 2010; published online 27 August 2010)

In this study, strong strain dependence of the elastic stiffness is found in polycrystalline Pt films. Epitaxial and polycrystalline Pt films thinner than 100 nm were deposited on monocrystal MgO substrates and resonance frequency of longitudinal standing wave in the film thickness direction was measured by picosecond ultrasound. In epitaxial Pt film, the resonance frequency was comparable to or smaller than the value expected from the elastic stiffness of bulk Pt, indicating softening of epitaxial Pt films, where nanoscale defects were observed: the softening was attributed to the defects. However, in polycrystalline Pt films, resonance frequency increased as the film thickness decreased and when the film thickness was smaller than 20 nm, the value exceeded the predicted value from the bulk stiffness, indicating the stiffening of the Pt film. Furthermore, resonance frequency showed good correlation with the strain. This trend is expected considering the higher elasticity. However, the slope between the resonance frequency and the strain is ten times as large as the value deduced from third-order elastic constant. © *2010 American Institute of Physics*. [doi:10.1063/1.3460799]

I. INTRODUCTION

Thin films often include nanoscale defects and residual stress, for which the elastic stiffness is different from that of bulk materials. The nanoscale defects include voids and weak bonds at grain boundaries, causing the softening.[1,2] In a highly strained condition, the elastic stiffness changes because of lattice anharmonicity, so called acoustoelasticity.[3,4] Surface effect is also a possible factor affecting the elastic stiffness. It stands for the lower symmetry at the surface[5,6] and it is considered that the surface tension and change in the electron density at the surface contribute the stiffening and softening of the films. Thus, there are several factors, but quantitative evaluation of their effects on the elastic stiffness has been never straightforward, being a long running problem. Elastic stiffness of thin film is a key parameter for designing band pass filters such as surface acoustic wave filters and film-bulk acoustic resonator; their center frequency depends on the elastic stiffness of construction materials such as piezoelectric films, oxide films, and metallic electrodes. Therefore, quantitative evaluation of elastic property of thin film is an important research topic both in scientific and practical fields.

For studying the elastic property of thin films, microtensile testing,[7,8] cantilever-bending-resonance method,[9] nanoindentation,[10] Rayleigh-wave velocity measurement,[11] and Brillouin scattering[12] have been used. These methods have contributed to investigate the isotropic or in-plane elastic stiffness of thin films. However, they are insensitive to the out-of-plane elastic stiffness and there are ambiguities in the relationship between the microstructure and elastic property in the out-of-plane direction. In this paper, for studying the elastic stiffness of metallic thin films, resonance frequency of longitudinal standing waves in the thickness direction is measured. The resonance frequency is closely related with the out-of-plane longitudinal-wave elastic stiffness and change in the resonance frequencies reflects the change in the elastic stiffness. For measuring the resonance frequencies, we apply the picosecond ultrasound. This method generates the longitudinal-wave phonons by the irradiation of the film with the femtosecond light pulse and they are preferentially detected by the probing pulse, which allows evaluating the elasticity of metallic thin films. Comparing with the other methods, this method is superior in term of noncontacting technique and being applicable to the ultrathin films, typically thinner than 100 nm thick.

In this study, we pay attention to epitaxial and polycrystalline Pt films deposited on MgO substrates. Pt thin film is a candidate for seed layers as well as electrodes,[13] on which magnetic films or single-crystal ceramic films are deposited. When Pt films are deposited on heated MgO substrates, Pt grows epitaxially and the orientation of the substrate determines the crystallographic orientation of the films. We systematically study the relationship between the microstructure and elastic stiffness for a variety of Pt films fabricated by varying the substrate temperature and substrate orientation.

II. EXPERIMENTS

We deposited Pt films on (001), (110), and (111) planes of single-crystal MgO substrates by rf-magnetron sputtering. Background pressure was less than 7.0×10^{-6} Pa, and during the deposition, Ar pressure was 0.8 Pa. Deposition rate was 1.8 Å/s. Epitaxial Pt films were deposited on the substrates heated up to 500 °C. After the deposition, temperature was kept at 500 °C for 15 min. It was then cooled down at the rate of 4 °C/min; at 200 °C, it was switched to the natural cooling in the vacuum chamber. Polycrystalline Pt films were fabricated by depositing Pt on (001), (110), and (111) planes of single-crystal MgO substrates at room tem-

[a]Electronic mail: nobutomo@me.es.osaka-u.ac.jp.

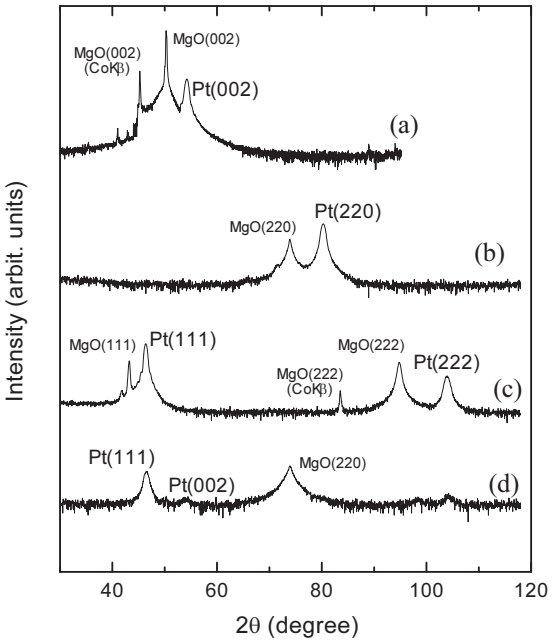

FIG. 1. X-ray diffraction spectra of (a) $Pt^{Epi}(001)/MgO(001)$ of 29.2 nm thick, (b) $Pt^{Epi}(110)/MgO(110)$ of 30.2 nm thick, (c) $Pt^{Epi}(111)/MgO(111)$ of 28.0 nm thick, and (d) $Pt^{Poly}(111)/MgO(110)$ film of 14.0 nm thick (CoK β). Vertical axis is logarithmic scale.

perature with the same pressure and deposition rate as epitaxial Pt films. Film thickness ranged from 8 to 97 nm, which was measured by the low-angle x-ray reflectivity measurements.[14,15]

In Fig. 1, it was confirmed that when Pt films were deposited at 500 °C, Pt(001), Pt(110), and Pt(111) epitaxial films were grown on MgO(001), MgO(110), and MgO(111) planes, respectively. In-plane x-ray diffraction measurements also confirmed the epitaxial growth. When Pt films were deposited at room temperature, ⟨111⟩-textured polycrystalline Pt films were grown on MgO(001), MgO(110), and MgO(111) planes. Significant film thickness dependence was not observed in the texture.

Figure 2 shows typical atomic force microscopy (AFM) images of the sputtered Pt films and the corresponding surface roughness, *Ra*. The AFM observations revealed that epitaxial Pt films showed grain structure and the shape of the grains depended on the orientation of MgO substrates: square grains grew on MgO(001) and ellipsoid grains on MgO(110). As the film thickness increased, the grain size increased; the grains came in contact with each other and

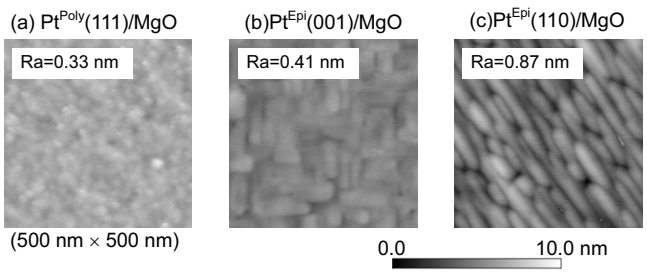

FIG. 2. AFM images and surface roughness, *Ra*, of (a) $Pt^{Poly}(111)/MgO$ film of 8.5 nm thick, (b) $Pt^{Epi}(001)/MgO(001)$ of 18.0 nm thick, and (c) $Pt^{Epi}(110)/MgO(110)$ of 18.9 nm thick.

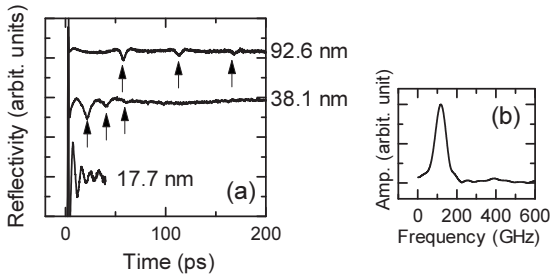

FIG. 3. (a) Time-resolved reflectivity change in the probe beam for $Pt^{Epi}(001)/MgO(001)$ films: arrows indicate the pulse-echo signals. (b) Fourier spectrum of the reflectivity change in $Pt^{Epi}(001)/MgO(001)$ of 17.7 nm thick.

coalescence occurred, making larger grains. In contrast, significant grain structure was not observed in polycrystalline Pt films, and they showed the dense structure.

Resonance frequency of longitudinal standing waves, $f_\perp$, was measured by the picosecond ultrasound.[16,17] When a film is relatively thin, irradiation of the film with the femtosecond light pulse excites the phonons with various wave numbers simultaneously, and longitudinal standing modes with frequency $f_\perp$ remains. According to the continuum dynamics, $f_\perp$ depends on the longitudinal elastic stiffness in the thickness direction, $C_\perp$, film thickness, d, and mass density, ρ,

$$f_\perp = \frac{n}{2d}\sqrt{\frac{C_\perp}{\rho}}, \tag{1}$$

where n denotes the mode index number, and the fundamental mode, $n=1$, was measured in this study. Because $f_\perp$ is proportional to the square root of $C_\perp$, $C_\perp$ is evaluated by measuring $f_\perp$. $f_\perp$ is determined from the reflectivity change in the probing light pulse reflected at the film surface. Details of our measurement setup appear elsewhere.[18,19]

III. RESULTS

Figure 3(a) shows the typical time-resolved reflectivity changes from $Pt^{Epi}(001)/MgO(001)$ films. When the film thickness was smaller than 35 nm, a standing wave was clearly detected, and $f_\perp$ was determined from the corresponding Fourier spectrum [Fig. 3(b)]. For the thicker films, the reflectivity change showed a train of echo signals, which indicated that coherent longitudinal-wave phonon pulses were generated near the film surface, propagated in the thickness direction with velocity, $v_\perp$, and reflected at the interface between the film and substrate. For these films, we estimated $f_\perp$ from $v_\perp$ as $f_\perp = v_\perp/(2d)$. $v_\perp$ was determined from the round-trip time, Δt, of acoustic pulse in the Pt film and d through $v_\perp = 2d/\Delta t$. Measured $f_\perp$ and $v_\perp$ reflects the phase velocity and group velocity, respectively. Therefore, for the thicker films, the calculated $f_\perp$ based on $v_\perp$ could be different from the actual value of $f_\perp$ because of the dispersion relation. However, we here ignore the effect of the dispersion, because the wave number is much smaller than the Brillouin zone boundary.

$f_\perp$ and normal strain in the thickness direction, $S_\perp$, of the Pt films are shown in Fig. 4. $f_\perp$ is normalized by the corresponding bulk value which is calculated by the Eq. (1)

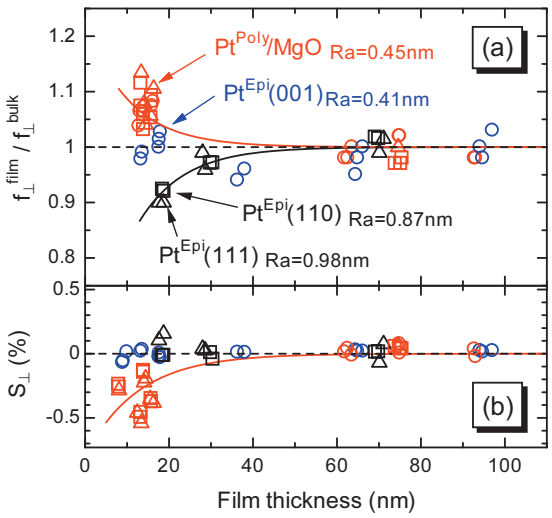

FIG. 4. (Color) Film thickness dependence of (a) resonance frequency of the longitudinal standing waves, $f_\perp$, and (b) normal strain in the thickness direction, $S_\perp$: open circles, squares, and triangles indicate that Pt films are deposited on (001), (110), and (111) planes of MgO, respectively.

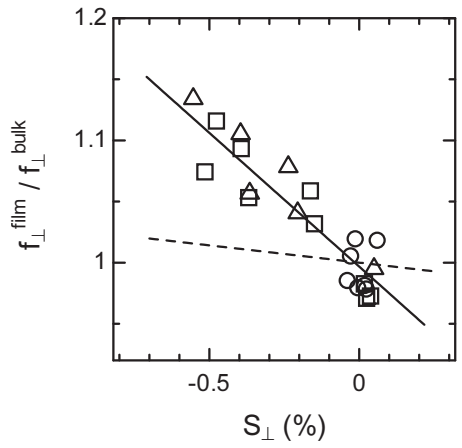

FIG. 5. Relationship between the resonance frequency, $f_\perp$, and the strain, $S_\perp$ in polycrystalline Pt films on MgO. A solid line shows the approximation curve and a dashed line the predicted strain dependence which is calculated from the third-order elasticity. Open circles, squares, and triangles indicate that Pt films are deposited on (001), (110), and (111) planes of MgO, respectively.

using the bulk values of $C_\perp$ (Ref. 20) and ρ. For $Pt^{Epi}(111)/MgO(111)$ and $Pt^{Poly}(111)/MgO$, longitudinal elastic stiffness in ⟨111⟩ direction of bulk Pt was used as $C_\perp$: $C_{Bulk}^{\langle 111\rangle}=(C_{11}+2C_{12}+4C_{44})/3=384.7$ GPa. For $Pt^{Epi}(001)/MgO(001)$ and $Pt^{Epi}(110)/MgO(110)$ films, the corresponding longitudinal elastic stiffness, $C_{Bulk}^{\langle 001\rangle}=C_{11}=346.7$ GPa and $C_{Bulk}^{\langle 110\rangle}=(C_{11}+C_{12}+2C_{44})/2=375.2$ GPa were used, respectively. $S_\perp$ was determined from the interplanar spacing of the films and the bulk Pt measured by the x-ray diffraction measurements. In polycrystalline Pt films, (111) direction of grains are preferentially oriented in the film thickness direction and deformation of the (111)-oriented grains governs the macroscopic deformation. Therefore, $S_\perp$ was deduced from the change in the (111) diffraction angle. *Ra* of typical Pt films around 18 nm thick is shown in Fig. 4(a).

IV. DISCUSSION

In epitaxial films, $f_\perp$ of $Pt^{Epi}(001)/MgO(001)$ was independent of the film thickness and was comparable to the corresponding bulk value. However, $f_\perp$ of $Pt^{Epi}(110)/MgO(110)$ and $Pt^{Epi}(111)/MgO(111)$ decreased as the film thickness decreased. In epitaxial films, $S_\perp$ is independent of the film thickness. Then, contribution of acoustoelasticity to the thickness dependence of $f_\perp$ must be negligibly small. Therefore, nanoscale defects should be a dominant factor which governs the elastic property. In AFM observations, $Pt^{Epi}(110)/MgO(110)$ and $Pt^{Epi}(111)/MgO(111)$ were defective comparing with the $Pt^{Epi}(001)/MgO(001)$. Larger *Ra* also supports this view. When the grains contact with each other, nanodefects (incohesive bonding regions and nanoscale voids) are formed at the grain boundaries. Such defects decrease the macroscopic elastic stiffness of films.[21,22] Volume fraction of grain-boundary regions is larger when the grain size is smaller. Therefore, smaller $f_\perp$ in $Pt^{Epi}(110)/MgO(110)$ and $Pt^{Epi}(111)/MgO(111)$ is attributed to larger volume fraction of nanoscale defects. Comparing them, $Pt^{Epi}(001)/MgO(001)$ was less defective and $f_\perp$ was comparable to the corresponding bulk value.

In $Pt^{Poly}(111)/MgO$, noteworthy elastic property was observed: $f_\perp$ increased as the film thickness decreased and when the film thickness was smaller than 20 nm, $f_\perp$ exceeded the corresponding bulk value. $S_\perp$ also showed the dependence on the film thickness; $S_\perp$ decreased as the film thickness decreased. These results were independent of the orientation of the MgO substrates. Defects can never explain the increment of $f_\perp$. If the Pt films include a number of defects and the mass density decreases, the larger $f_\perp$ is explained through Eq. (1). However, as seen in $f_\perp$ of epitaxial Pt films, $f_\perp$ of defective films is usually smaller than the corresponding bulk value, because elastic stiffness is much sensitive to the defects. For this reason, change in the mass density is not a dominant factor for the larger $f_\perp$. In polycrystalline films, change in the crystallographic orientation affects the macroscopic elastic stiffness. In Fig. 4, $f_\perp$ of $Pt^{Poly}(111)/MgO$ is normalized by $f_\perp$ calculated using the longitudinal elastic stiffness in the (111) direction. In typical fcc materials, elastic stiffness becomes a maximum in the (111) direction, and the calculated $f_\perp^{Bulk}$ is the maximum possible value in Pt. Therefore, change in the orientation cannot explain the enhancement of $f_\perp$. In Fig. 5, $f_\perp$ obviously shows the relationship with the $S_\perp$, and this indicates that the acoustoelasticity is a possible reason of the enhanced $f_\perp$.

We here evaluate the strain dependence of the elastic stiffness using third-order elastic constants. When residual strain exists in a material, elastic stiffness is different from that in unstrained materials; compressive strain increases the corresponding stiffness and tensile strain decreases. We deduced the strain dependence of $C_\perp$ by calculating $(\partial C_\perp/\partial S_\perp)/C_\perp$ following previous studies.[3,19] In this calculation, we assumed that the thin films were extended biaxially along the in-plane directions, and they shrink in the film thickness direction because of Poisson's effect. Because of the (111) texture in polycrystalline Pt films, we calculated

elastic stiffness in [111] direction by applying the stress in $[1\bar{1}0]$ and $[11\bar{2}]$ directions. This calculation confirmed that the strain dependence, $(\partial C_{\perp}^{\langle 111\rangle}/\partial S_{\perp}^{\langle 111\rangle})/C_{\perp}^{\langle 111\rangle}$, becomes -5.7. In this calculation, we used the reported second-order and third-order elastic constants of bulk Pt.[23] From the calculated $(\partial C_{\perp}^{\langle 111\rangle}/\partial S_{\perp}^{\langle 111\rangle})/C_{\perp}^{\langle 111\rangle}$, strain dependence of $f_{\perp}$ is calculated, and it is shown by a dashed line in Fig. 5. Slope of the dashed line, $(f_{\perp}^{\mathrm{film}}/f_{\perp}^{\mathrm{bulk}})/S_{\perp}=-2.4$, is smaller than that of the observed relationship (a solid line in Fig. 5), $(f_{\perp}^{\mathrm{film}}/f_{\perp}^{\mathrm{bulk}})/S_{\perp}=-21.9$, and acoustoelasticity of the bulk Pt fails to explain the observation quantitatively. If the third-order elastic constants were ten times as large as the reported values, the observation would be consistently explained.

One of the possible reasons that cause the mismatch between the measured and calculated strain dependences of $f_{\perp}$ is the errors in the reported third-order elastic constants. Third-order elastic constants of the bulk materials are usually measured with applying the static strain to the materials. Although the measurement accuracy is improved as the applied stress increases, the applied strain is typically less than 0.01% to prevent the dislocation movements,[4] which is necessarily large enough to determine them accurately. Actually, the third-order elastic constants of bulk Pt have not been measured and we used the calculated values in the above discussion. Therefore, the actual third-order elastic constants of Pt could be larger than the reported values.

V. CONCLUSIONS

Whether elastic stiffness of nanoscale composites is stiffer or softer is a long running problem. In this study, we found that polycrystalline Pt films on MgO are stiffened and the resonance frequency highly depends on the $S_{\perp}$. There are several factors that affect the macroscopic elastic stiffness of nanoscale components. However, they failed to explain the strain-dependent elastic stiffness quantitatively. This result proposes a challenging topic on theoretical study.

[1] N. Nakamura, H. Ogi, and M. Hirao, Acta Mater. **52**, 765 (2004).
[2] H. Ogi, N. Nakamura, H. Tanei, M. Hirao, R. Ikeda, and M. Takemoto, Appl. Phys. Lett. **86**, 231904 (2005).
[3] R. N. Thurston and K. Brugger, Phys. Rev. **133**, A1604 (1964).
[4] Y. Hiki and A. V. Granato, Phys. Rev. **144**, 411 (1966).
[5] S. Cuenot, C. Frétigny, S. Demoustier-Champagne, and B. Nysten, Phys. Rev. B **69**, 165410 (2004).
[6] G. Y. Jing, H. L. Duan, X. M. Sun, Z. S. Zhang, J. Xu, Y. D. Li, J. X. Wang, and D. P. Yu, Phys. Rev. B **73**, 235409 (2006).
[7] K. F. Badawi, P. Villain, Ph. Goudeau, and P.-O. Reault, Appl. Phys. Lett. **80**, 4705 (2002).
[8] A. Cervellino, P. M. Derlet, and H. Van Swygenhoven, Acta Mater. **54**, 1851 (2006).
[9] H. Mizubayashi, T. Yamaguchi, W. Song, A. Yamaguchi, and R. Yamamoto, J. Alloys Compd. **211–212**, 442 (1994).
[10] R. Saha and W. D. Nix, Acta Mater. **50**, 23 (2002).
[11] J. B. Rubin and R. B. Schwarz, Phys. Rev. B **50**, 795 (1994)′.
[12] C. Rossignol, B. Perrin, B. Bonello, P. Djemia, P. Moch, and H. Hurdequint, Phys. Rev. B **70**, 094102 (2004).
[13] J. Son, J. Cagnon, D. S. Boesch, and S. Stemmer, Appl. Phys. Express **1**, 061603 (2008).
[14] H. Kiessig, Ann. Phys. **402**, 769 (1931).
[15] L. G. Parratt, Phys. Rev. **95**, 359 (1954).
[16] C. Thomsen, J. Strait, Z. Vardeny, H. J. Maris, J. Tauc, and J. J. Hauser, Phys. Rev. Lett. **53**, 989 (1984).
[17] C. Thomsen, H. T. Grahn, H. J. Maris, and J. Tauc, Phys. Rev. B **34**, 4129 (1986).
[18] H. Ogi, M. Fujii, N. Nakamura, T. Shagawa, and M. Hirao, Appl. Phys. Lett. **90**, 191906 (2007).
[19] H. Ogi, M. Fujii, N. Nakamura, T. Yasui, and M. Hirao, Phys. Rev. Lett. **98**, 195503 (2007).
[20] R. E. Macfarlane, J. A. Rayne, and C. K. Jones, Phys. Lett. **18**, 91 (1965).
[21] H. Tanei, N. Nakamura, H. Ogi, M. Hirao, and R. Ikeda, Phys. Rev. Lett. **100**, 016804 (2008).
[22] H. Tanei, K. Tanigaki, K. Kusakabe, H. Ogi, N. Nakamura, and M. Hirao, Appl. Phys. Lett. **94**, 041914 (2009).
[23] S. S. Mathur and P. N. Gupta, Acustica **31**, 114 (1974).